

## Role of Singlet Diradicals in Reactions of 2-Carbenabicyclo[3.2.1]octa-3,6-diene

Peter K. Freeman and James K. Pugh

Department of Chemistry, Oregon State University, Corvallis, Oregon 97331

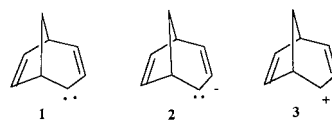
peter.freeman@orst.edu

Received December 14, 2000

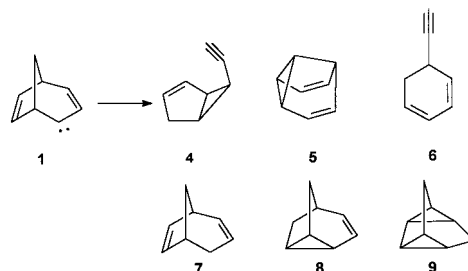
The generation of 2-carbenabicyclo[3.2.1]octa-3,6-diene (**1**) results in the formation of C<sub>8</sub>H<sub>8</sub> hydrocarbons endo-6-ethynylbicyclo[3.1.0]hex-2-ene (**4**), semibullvalene (**5**), and 5-ethynyl-1,3-cyclohexadiene (**6**), and C<sub>8</sub>H<sub>10</sub> hydrocarbons bicyclo[3.2.1]octa-2,6-diene (**7**), tricyclo[3.2.1.0<sup>4,6</sup>]oct-2-ene (**8**), and tetracyclo[3.3.0.0<sup>2,8</sup>.0<sup>4,6</sup>]octane (**9**). Focus is placed on three mechanistic pathways for the formation of the C<sub>8</sub>H<sub>10</sub> hydrocarbon fraction: (a) abstraction of hydrogen by triplet carbene **1T** to produce an equilibrating set of monoradicals, (b) interconversion of triplet carbene **1T** into tricyclic triplet diradical **19T** and tetracyclic triplet diradical **20T**, and (c) interconversion of singlet **1S** with analogous singlet diradical **19S** and **20S**. Ab initio calculations at the (U)B3LYP/6-311+G-(3df,2p)/(U)B3LYP/6-31G(d,p) and broken spin symmetry UBS B3LYP/6-311+G(3df,2p)/B3LYP/6-31G(d,p) levels rule out choices (a) and (b) and are consistent with the singlet diradical process.

2-Carbenabicyclo[3.2.1]octa-3,6-diene (**1**) has provoked our interest because it has the potential for either homoaromaticity or antihomoaromaticity. It might resemble the homoaromatic anion (**2**) or the antihomoaromatic cation (**3**) depending on whether the nonbonding carbene carbon electrons move into the  $\pi$  system to make it a six- $\pi$ -electron system or stay essentially in an sp<sup>2</sup> orbital (Scheme 1). Ab initio calculations of structure, stabilization energy, magnetic properties, the triplet–singlet energy gap, and the relation of these features to those of model systems suggest that 2-carbenabicyclo[3.2.1]octa-3,6-diene (**1**) is antihomoaromatic.<sup>1,2</sup> As an intermediate, bivalent **1** travels through a variety of pathways to product, forming endo-6-ethynylbicyclo[3.1.0]hex-2-ene (**4**), semibullvalene (**5**), 5-ethynyl-1,3-cyclohexadiene (**6**), bicyclo[3.2.1]octa-2,6-diene (**7**), tricyclo[3.2.1.0<sup>4,6</sup>]oct-2-ene (**8**), and tetracyclo[3.3.0.0<sup>2,8</sup>.0<sup>4,6</sup>]octane (**9**) (Scheme 2).<sup>3</sup> The formation of ethynylbicyclohexene **4** is of particular interest because formation of **4** is an outcome favored by isomeric intermediates bicyclic allene **10** and tetracyclic carbene **11**.<sup>4,5</sup> Thus, a reaction manifold involving intermediates **1**, **10**, and **11**, with formation of ethynylbicyclohexene **4** either directly or indirectly from each intermediate, is possible (Scheme 3). Ab initio calculations of the transition structures at the B3LYP/6-31G(d,p) level for all the transformations indicated in Scheme 3 reveal that each intermediate proceeds directly to product without participation in the **1**  $\rightleftharpoons$  **10**  $\rightleftharpoons$  **11**

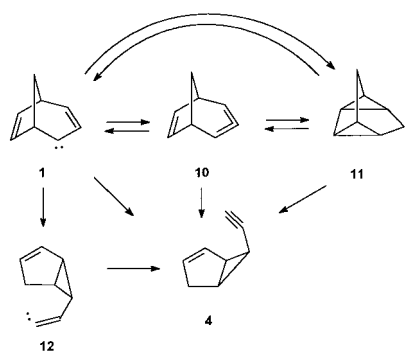
Scheme 1



Scheme 2



Scheme 3



manifold, with carbenabicyclooctadiene forming **4** via a retro divinylcyclopropane rearrangement to vinylidene carbene **12**, which undergoes a 1,2-hydrogen shift to complete the process.<sup>6</sup> Formation of semibullvalene **5** is an example of  $\gamma$ -C–H insertion (Scheme 4), while formation of ethynylcyclohexadiene **6** may involve a carbene-to-carbene rearrangement followed by a cyclopropylcar-

(1) Freeman, P. K.; Pugh, J. K. *J. Org. Chem.* **2000**, *65*, 6107–6111.

(2) Freeman, P. K. *J. Am. Chem. Soc.* **1998**, *120*, 1619–1620.

(3) Freeman, P. K.; Swenson, K. E. *J. Org. Chem.* **1982**, *47*, 2033–2039.

(4) Balci, M.; Jones, W. M. *J. Am. Chem. Soc.* **1981**, *103*, 2874–2876.

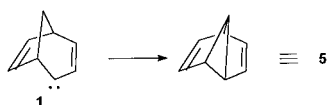
(5) Bergman, R. G.; Rajadhyaksha, V. J. *J. Am. Chem. Soc.* **1970**, *92*, 2163–2164.

(6) Freeman, P. K.; Pugh, J. K. *J. Am. Chem. Soc.* **1999**, *121*, 2269–2273.

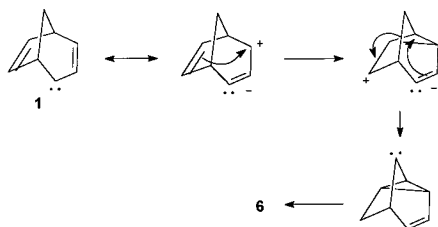
(7) Freeman, P. K.; Balls, D. M. *J. Org. Chem.* **1967**, *32*, 2354–2356.

(8) Freeman, P. K.; Kuper, D. G. *J. Org. Chem.* **1965**, *30*, 1047–1049.

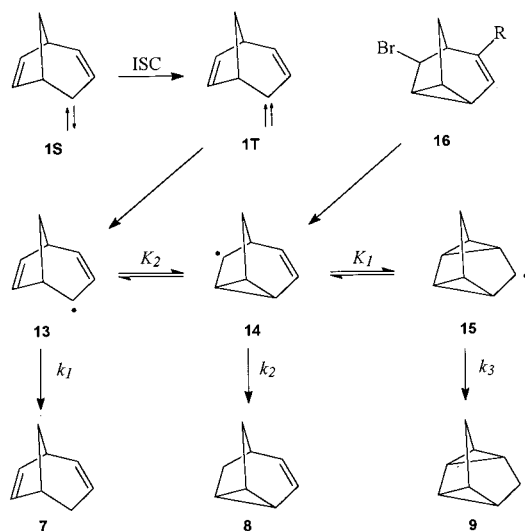
Scheme 4



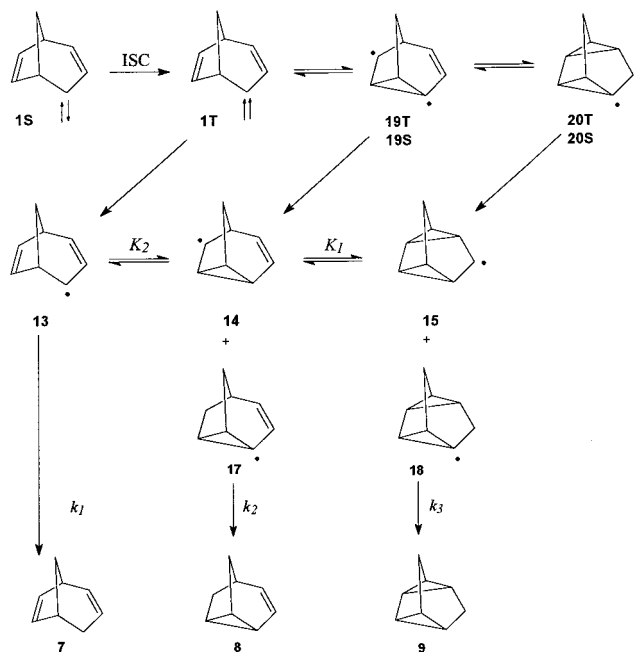
Scheme 5



Scheme 6



Scheme 7



ene fragmentation<sup>7-16</sup> (Scheme 5). The products generated from carbenabicyclooctadiene **1** consist of two groups: the first, consisting of **4**, **5**, and **6**, are all C<sub>8</sub>H<sub>8</sub> species; the second is comprised of polycyclic **7**, **8**, and **9**, which are all C<sub>8</sub>H<sub>10</sub> species. Our purpose here is to develop an improved understanding of the mechanistic pathways involved in the formation of these species in the second group, each of which has picked up two additional hydrogens.

Our earlier study of carbenabicyclooctadiene **1** revealed that the triplet is the ground state,<sup>1</sup> so at first glance, a reasonable suggestion is that singlet **1S** undergoes intersystem crossing to form triplet **1T** that then abstracts hydrogen to form radical **13**, which in turn sets up an equilibrium of **13**, **14**, and **15** (Scheme 6). In the generation of hydrocarbons **7**, **8**, and **9**, the composition always provides substantial amounts of components **8** and **9** (e.g., from precursor tosylhydrazone with KH/18-

crown-6, diglyme **7:8:9** = 19:12:10).<sup>3</sup> Assuming that the rates of hydrogen abstraction for the second abstraction step are similar, we can rule out this scenario because Klumpp and co-workers<sup>17</sup> found that treatment of **16** (R = D) with tri-*n*-butyltin hydride or with sodium in *tert*-butyl alcohol formed only monodeuterio diene **7**. Using these same free-radical conditions with **16** (R = H), we found no detectable tetracyclic **9** (with <sup>*n*</sup>Bu)<sub>3</sub>SnH, **7:8:9** = 98.7:1.3:<0.1, and with Na/*t*-BuOH, **7:8:9** = 97.5:2.5:<0.1).

There are many factors that could affect the ratio of products **7**, **8**, and **9**. The entry point into the rearrangement manifold, the equilibrium constants  $K_1$  and  $K_2$ , and the rates of hydrogen abstraction  $k_1$ ,  $k_2$ , and  $k_3$  could each play a role in product formation. It should be safe to assume, however, that the relative rates of hydrogen abstraction ( $k_1$ ,  $k_2$ , and  $k_3$ ) are equal in this type of system.<sup>18-20</sup> The analysis, therefore, is drawn principally by consideration of the equilibria between the radical species. If equilibration between the three radicals is not complete, then hydrocarbon **8** would be formed in excess from the tri-*n*-butyltin hydride or Na/*t*-BuOH reaction with bromide **16**. This would set an upper limit of 2.5% for the formation of **8** from the analogous carbene reaction. If the radical species are in equilibrium, then the product ratio from the carbene reaction should equal that observed from the radical generation from bromide **16**. Clearly, there is another mechanism in operation. A second variation on a triplet process involves a series of triplet diradicals as presented in Scheme 7. The singlet carbene could undergo intersystem crossing to give a triplet carbene species. The triplet carbene could then form a series of triplet diradical intermediates. Each of these could abstract a hydrogen to form the five radicals **13-15**, **17**, and **18**. An equilibrium could be established

(9) Guarino, A.; Wolf, A. P. *Tetrahedron Lett.* **1969**, 655-658.

(10) Berson, J. A.; Bauer, W.; Campbell, M. M. *J. Am. Chem. Soc.* **1970**, *92*, 7515-7517.

(11) Jones, M., Jr.; Reich, S. D. *J. Am. Chem. Soc.* **1967**, *89*, 3935-3936.

(12) Kirmse, W.; Pook, K.-H. *Chem. Ber.* **1965**, *98*, 4022-4027.

(13) Friedman, L.; Shechter, H. *J. Am. Chem. Soc.* **1960**, *82*, 1002-1003.

(14) Sauer, R. R.; Schlosberg, S. B.; Pfeffer, P. E. *J. Org. Chem.* **1968**, *33*, 2175-2181.

(15) Lemal, D. M.; Fry, A. J. *J. Org. Chem.* **1964**, *29*, 1673-1676.

(16) Cristol, S. J.; Harrington, J. K. *J. Org. Chem.* **1963**, *28*, 1413-1415.

(17) Japenga, J.; Klumpp, G. W.; Stapersma, J. *Tetrahedron* **1977**, *33*, 2847-2849.

(18) Warner, C. R.; Strunk, R. J.; Kuivila, H. G. *J. Org. Chem.* **1966**, *31*, 1, 3381-3384.

(19) Martin, M. M.; DeJongh, D. C. *J. Am. Chem. Soc.* **1962**, *84*, 3526-3531.

(20) Wilt, J. W.; Levin, A. A. *J. Org. Chem.* **1962**, *27*, 2319-2322.

**Table 1. Energies of Diradical Species**

structure	B3LYP/6-31G(d,p) <sup>a</sup>	$\langle S^2 \rangle^b$	B3LY/6-311+G(3df,2p) <sup>c</sup>	$\langle S^2 \rangle^b$	ZPE <sup>d</sup>	ZPE <sup>f</sup>	relative energy <sup>g</sup> B3LYP/6-31G(d,p)	relative energy <sup>h</sup> B3LYP/6-311+G(3df,2p)
<b>1T</b>	-309.510677	2.04	-309.598474	2.04	0.132643	0.129216	0	0
<b>19T</b>	-309.486264	2.01	-309.573078	2.01	0.131298	0.129361	14.5 [15.4]	15.1 [16.0]
<b>20T</b>	-309.478624	2.01	-309.563419	2.01	0.131693 <sup>e</sup>	0.130387	19.5 [20.9]	21.4 [22.7]
<b>1S</b>	-309.498743		-309.588874		0.132382		7.3	5.9
	(-309.502749)	0.65	(-309.591921)	0.60	(0.13185)		(4.5)	(3.6)
<b>19S</b>	-309.498157		-309.587265		0.131681		7.2	6.4
	(-309.499741)	0.49	(-309.587276)	0.37	(0.131235)		(6.0)	(6.1)
<b>20S</b>	-309.508263		-309.594443		0.133605		2.1	3.1

<sup>a</sup> Energies in au from UB3LYP/6-31G(d,p)//UB3LYP/6-31G(d,p) for triplets and restricted B3LYP/6-31G(d,p)//B3LYP/6-31G(d,p) and UBS at these levels in parentheses for singlets. <sup>b</sup> Spin expectation values for the triplets and broken spin symmetry singlets. <sup>c</sup> Energies in au from UB3LYP/6-311+G(3df,2p)//UB3LYP/6-31G(d,p) for triplets, and restricted B3LYP/6-311+G(3df,2p)//B3LYP/6-31G(d,p) and UBS at these levels in parentheses for singlets. <sup>d</sup> ZPE from (U)B3LYP/6-31G(d,p) and UBS B3LYP/6-31G(d,p) (in parentheses) frequency calculations on (U)B3LYP/6-31G(d,p)- and UBS B3LYP/6-31G(d,p)-optimized geometries. <sup>e</sup> Converged on only maximum force and RMS force. <sup>f</sup> ZPE from UHF/6-31G\*/UHF/6-31G\* calculations (scaling factor = 0.9135). <sup>g</sup> Relative energy in kcal/mol as given by (U)B3LYP/6-31G(d,p)//(U)B3LYP/6-31G(d,p)+ZPE at the same level; values in brackets employ ZPE at UHF/6-31G\*/UHF/6-31G\*; values in parentheses employ UBS B3LYP/6-31G(d,p)//B3LYP/6-31G(d,p)+ZPE at the same level. <sup>h</sup> Relative energy in kcal/mol as given by ((U)B3LYP/6-311+G(3df,2p)//(U)B3LYP/6-31G(d,p)+ZPE((U)B3LYP/6-31G(d,p))); values in brackets employ ZPE at UHF/6-31G\*/UHF/6-31G\*; values in parentheses employ UBS B3LYP/6-311+G(3df,2p)//B3LYP/6-31G(d,p)+ZPE at UBS B3LYP/6-31G(d,p).

**Table 2. Energies of Radical Species**

structure	UB3LYP/6-31G(d,p) <sup>a</sup>	UB3LYP/6-311+G(3df,2p) <sup>b</sup>	ZPE <sup>c</sup>	relative energy <sup>d</sup> UB3LYP/6-31G(d,p)	relative energy <sup>e</sup> UB3LYP/6-311+G(3df,2p)
<b>13</b>	-310.193301	-310.281523	0.144865	0	0
<b>14</b>	-310.172790	-310.259666	0.144837	12.9	13.7
<b>15</b>	-310.164605	-310.295444	0.144648	17.9	20.0

<sup>a</sup> Energies in au from UB3LYP/6-31G(d,p)//UB3LYP/6-31G(d,p). <sup>b</sup> Energies in au from UB3LYP/6-311+G(3df,2p)//UB3LYP/6-31G(d,p). <sup>c</sup> ZPE from UB3LYP/6-31G(d,p) frequency calculations on UB3LYP/6-31G(d,p)-optimized geometries. <sup>d</sup> Relative energy in kcal/mol as given by UB3LYP/6-31G(d,p)//UB3LYP/6-31G(d,p)+ZPE. <sup>e</sup> Relative energy in kcal/mol as given by UB3LYP/6-311+G(3df,2p)//UB3LYP/6-31G(d,p)+ZPE (UB3LYP/6-31G(d,p)).

among radicals **13**–**15**, whereas radicals **17** and **18** cannot equilibrate and would have to proceed directly to product. More formation of **8** and **9** would be expected from this mechanism than from a scenario limited to the equilibration of **13**–**15** as in Scheme 6. To examine the feasibility of this triplet diradical mechanism, DFT calculations at the UB3LYP/6-311+G(3df,2p)//UB3LYP/6-31G(d,p) level<sup>21</sup> were conducted on triplet diradical species **1T**, **19T**, and **20T** to compare the relative energies of the three. Recent reports from Houk and co-workers,<sup>22–24</sup> Bettinger et al.,<sup>25</sup> Abe et al.,<sup>26</sup> Sheridan and co-workers,<sup>27</sup> and this laboratory<sup>1</sup> demonstrate that the B3LYP method works well for diradicals and singlet and triplet carbenes using either the 6-31G\* or 6-31G\*\* basis set. The DFT calculations for the key intermediates of Scheme 7 are presented in Tables 1 and 2 and Figures 1 and 2.

The first point that can be made from the given energies (Table 2) is that there would not be an equilib-

rium among free radicals **13**–**15** as outlined in Scheme 7. Radical **13** is lower in energy than **14** and **15** by 13.7 and 20.0 kcal/mol, respectively. This would be enough of an energy difference to result in the formation of product solely from radical **13**. These computational results fit nicely with the experimental reaction composition derived from the formation of the radical species by tri-*n*-butyltin hydride and Na/*t*-BuOH. This also means that for the carbene reaction the relative product ratios must be anticipated in some manner before the first hydrogen abstraction by triplet **1T** leading to radical formation. The same argument, however, can be made against a role for an equilibrating set of triplet diradical species **1T**, **19T**, and **20T**. Triplet **1T** is 15.1 and 21.4 kcal/mol lower in energy than **19T** and **20T**, respectively, as shown in Table 1; however, the frequency calculation for **20T** at the UB3LYP/6-31G(d,p)//UB3LYP/6-31G(d,p) level only converged on maximum force and RMS force. A check of the results using zero point energies calculated at the UHF/6-31G\*/UHF/6-31G\* level, however, provided the same picture with **1T** lower in energy than **19T** and **20T** by 16.0 and 22.7 kcal/mol, respectively. Again, this difference is large enough that the only product that should be seen is hydrocarbon **7** formed from radical **13**. Perhaps the temperature is changing the energetic picture. The tosylhydrazone degradation was conducted at 120 °C; however, the relative energies of **1T**, **19T**, and **20T** are essentially unchanged at the UB3LYP/6-31G\*\* level calculated at 120 °C. At this point we turned our attention to the same diradical manifold but with respect to the singlet state rather than the triplet state. The calculations on singlets **1S**, **19S**, and **20S** were carried out using restricted B3LYP/6-31G(d,p) and B3LYP/6-311+G(3df,2p) methods and broken spin symmetry UBS methods at these same levels to provide additional accommodation for the potentially multiconfigurational

(21) Frisch, M. J.; Trucks, G. W.; Schlegel, H. B.; Gill, P. M. W.; Johnson, B. G.; Robb, M. A.; Cheeseman, J. R.; Keith, T.; Petersson, G. A.; Montgomery, J. A.; Raghavachari, K.; Al-Laham, M. A.; Zakrzewski, V. G.; Ortiz, J. V.; Foresman, J. B.; Cioslowski, J.; Stefanov, B. B.; Nanayakkara, A.; Challacombe, M.; Peng, C. Y.; Ayala, P. Y.; Chen, W.; Wong, M. W.; Andres, J. L.; Replogle, E. S.; Gomperts, R.; Martin, R. L.; Fox, D. J.; Binkley, J. S.; Defrees, D. J.; Baker, J.; Stewart, J. P.; Head-Gordon, M.; Gonzalez, C.; Pople, J. A. *GAUSSIAN 94, Revision B.2*; Gaussian, Inc.: Pittsburgh, PA, 1995.

(22) Goldstein, E.; Beno, B.; Houk, K. N. *J. Am. Chem. Soc.* **1996**, *118*, 6036–6043.

(23) Beno, B. R.; Wilsey, S.; Houk, K. N. *J. Am. Chem. Soc.* **1999**, *121*, 4816–4826.

(24) Houk, K. N.; Nendel, M.; Wiest, O.; Storer, J. W. *J. Am. Chem. Soc.* **1997**, *119*, 10545–10546.

(25) Bettinger, H. F.; Schleyer, P. v. R.; Schreiner, P. R.; Schaefer, H. F. Computational Analyses of Prototype Carbene Structures and Reactions. In *Modern Electronic Structure Theory and Applications in Organic Chemistry*, Davidson, E. R., Ed.; World Scientific: Singapore, 1997.

(26) Abe, M.; Adam, W.; Nau, W. M. *J. Am. Chem. Soc.* **1998**, *120*, 11304–11310.

(27) Subhan, W.; Rempala, P.; Sheridan, R. S. *J. Am. Chem. Soc.* **1998**, *120*, 11528–11529.

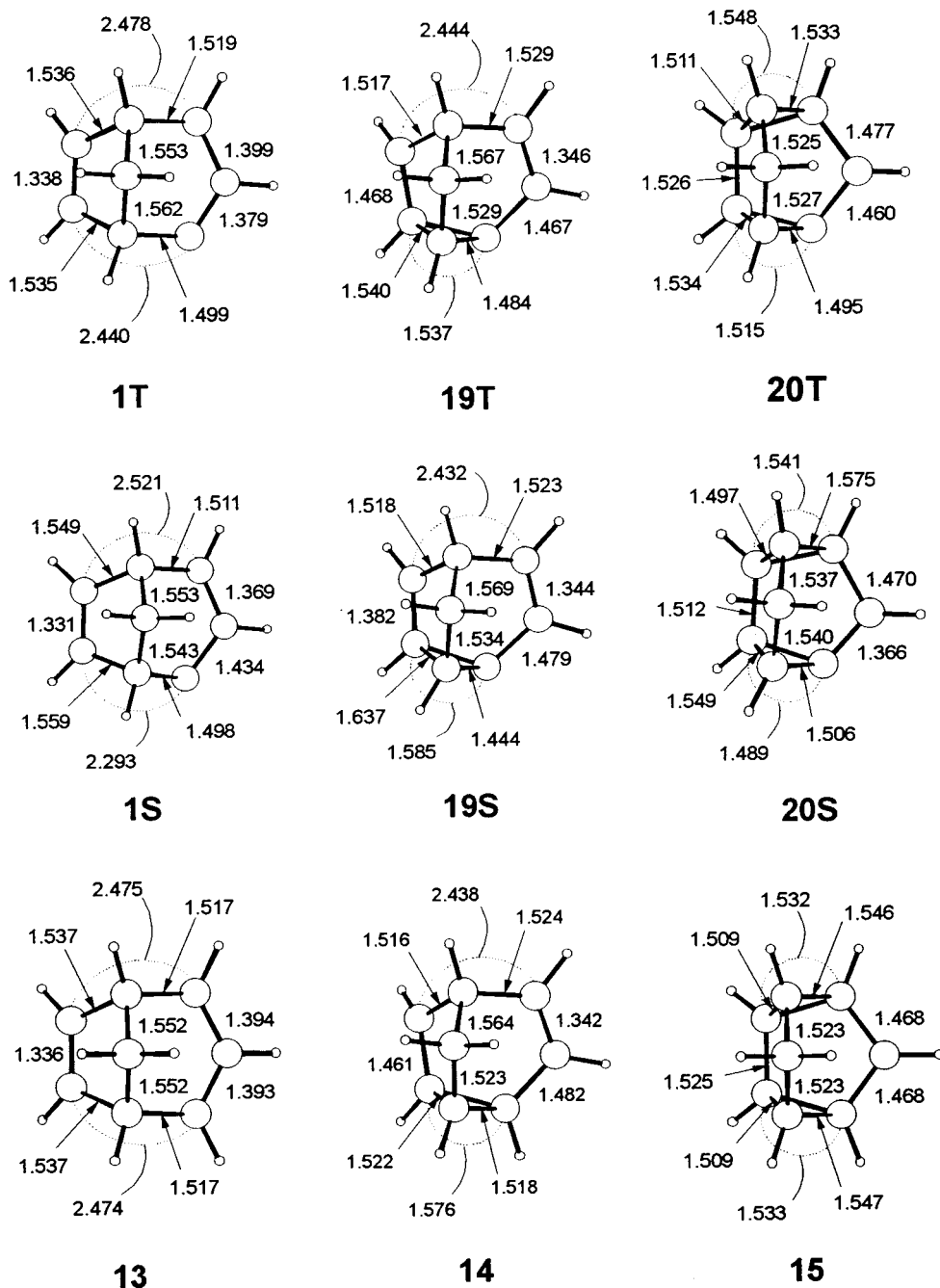


**Figure 1.** Structures for triplet and singlet carbenes **1T** and **1S**, triplet diradicals **19T** and **20T**, singlet diradicals **19S** and **20S**, and monoradicals **13–15**, all at the (U)B3LYP/6-31G(d,p)//(U)B3LYP/6-31G(d,p) level.

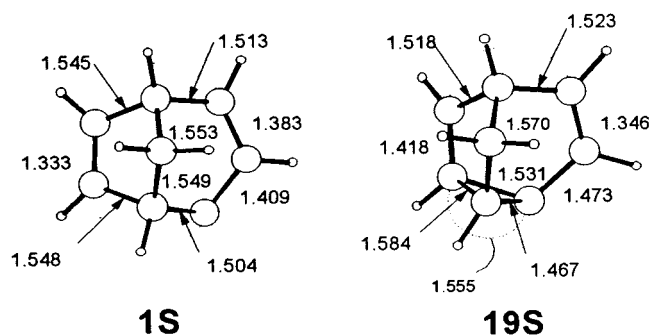
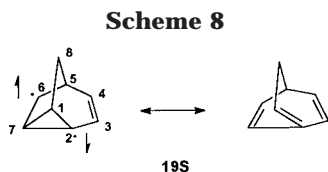


**Figure 2.** Structures for singlets **1S** and **19S** at the UBS B3LYP/6-31G(d,p)//B3LYP/6-31G(d,p) level.

nature of these species.<sup>28</sup> The energies of the singlet species **1S**, **19S**, and **20S** are much closer than those of

the corresponding triplets **1T**, **19T**, and **20T** with both restricted and broken spin symmetry UBS treatments. At the RB3LYP/6-311+G(3df,2p)//RB3LYP/6-31G(d,p) level, the energies relative to triplet **1T** are 5.9, 6.4, and 3.1; those at the UBS B3LYP/6-311+G(3df,2p)//B3LYP/6-31G(d,p) level are 3.6, 6.1, and 3.1 (Table 1). As **1S** and **19S** are close in energy with **20S** (the most stable), and since the entry point is **1S**, the production of hydrocarbons **8** and **9** can then be explained by a singlet diradical rearrangement manifold. Alternatively, the abundance of **7** in the carbene reaction can be explained by the singlet–triplet gap of **1**. The triplet (**1T**) is 5.9 (RB3LYP)

(28) Cramer, C. J. *J. Am. Chem. Soc.* **1998**, *120*, 6261–6269. Gräfenstein, J.; Hjerpe, A. M.; Kraka, E.; Cremer, D. *J. Phys. Chem. A* **2000**, *104*, 1748–1761. Kraka, E.; Cremer, D. *J. Am. Chem. Soc.* **2000**, *122*, 8245–8264. Schreiner, P. R.; Prall, M. *J. Am. Chem. Soc.* **1999**, *121*, 8615–8627.



or 3.6 kcal/mol (UBS B3LYP) lower in energy than the singlet (**1S**). The final product ratio can be explained by a combination of two competing processes. Formation of triplet **1T** is energetically favorable and would give product **7**. Products **8** and **9** stem from the singlet diradical manifold.

The singlet diradicals **19S** and **20S** are key intermediates in the favored reaction scheme. They are both more stable than their triplet counterparts, and a consideration of structural differences may provide hints as to why. In the case of singlet **19S**, the broken spin symmetry UBS calculation lowers the energy by 0.3 kcal/mol (Table 1). At the RB3LYP and UBS B3LYP/6-31G(d,p) levels, we

find short C6–C7 (1.382 and 1.418 Å) and C1–C2 bonds (1.444 and 1.467 Å) and long C1–C7 (1.637 and 1.584 Å) and C2–C7 bonds (1.585 and 1.555 Å) relative to those of the triplet (with 1.468, 1.484, 1.540, and 1.537 Å, respectively) (Figures 1 and 2). This can be ascribed to the cyclopropylcarbinyl radical resonance that is favored only in the singlet due to spin restrictions (Scheme 8). The singlet **20S** is stable to spin symmetry breaking due to its non-multiconfigurational nature. It is noteworthy that **20S** exhibits a short C2–C3 bond (1.366 Å) relative to that of the triplet **20T** (1.460 Å) and thus considerable double-bond character at this location.

**Acknowledgment.** We thank Professors Dieter Cremer and John Loeser for helpful discussions and acknowledge with thanks the support from the Oregon State University Research Council, the MRF fund, and NIEHS.

JO001745Q